

## Relativistic theory for the nuclear spin-lattice relaxation rate in ferromagnetic metals with application to 5d impurities in bcc Fe

I. Cabria, M. Deng, and H. Ebert

*Institut für Physikalische Chemie, Universität München, Butenandtstraße 5-13, D-81377 München, Germany*

(Received 16 November 1999)

A relativistic theory for the nuclear spin-lattice relaxation rate  $(TT_1)^{-1}$  in ferromagnetic metals is presented that includes in particular the electric quadrupolar and the core polarization contributions. Because it is formulated within the framework of the spin-polarized relativistic version of the Korringa-Kohn-Rostoker method of band structure calculations it can be applied in principle to any kind of system. Here an application of the theory to 5d impurities (Lu–Hg) in ferromagnetic bcc Fe is presented. While the core polarization contribution turned out to be negligible in all cases, the electric quadrupolar contribution was found to be of the same order of magnitude as the magnetic dipolar one in the case of Lu, Hf, Ir, and Au.

### I. INTRODUCTION

The magnetic hyperfine field and the nuclear spin-lattice relaxation rate  $R$  are the most prominent hyperfine interaction parameters for ferromagnetic solids. While the first quantity is a ground-state property, the second one is related to low-lying excitations at the Fermi level. Previous theoretical investigations for paramagnetic systems have shown that if electron-electron interaction is ignored,  $R$  can be expressed in terms of the squared angular momentum resolved density of states (DOS) at the Fermi energy. For that reason the relaxation rate is a very sensitive probe for the electronic structure around the Fermi level, and a small perturbation on the DOS could easily change  $R$  by an order of magnitude. This implies that a realistic and reliable approach must be used to calculate  $R$ , a goal that has been reached in several steps during the last decades.

Heitler and Teller were the first who discussed the most prominent spin-lattice relaxation mechanism in metals: the magnetic interaction between the nuclei and the conduction electrons.<sup>1</sup> The theory of the nuclear spin relaxation process and the main driving mechanisms were clarified in the following years<sup>2–7</sup> and after that, a lot of estimations and calculations of the relaxation rate were done. On the basis of scalar relativistic linear muffin-tin orbitals (LMTO) band structure calculations, several authors calculated the relaxation rate in pure cubic and hexagonal closed packed (hcp) transition metals.<sup>8–15</sup> Masuda *et al.*<sup>16</sup> made estimations for the relaxation rate of 3d, 4d, and 5d transition impurities in bcc Fe, based on the theoretical work by Moriya.<sup>17</sup> Kanamori and co-workers made *ab initio* calculations of relaxation rates of impurities in bcc Fe.<sup>18</sup> These calculations were improved and extended by Akai *et al.* using the spin-polarized Korringa-Kohn-Rostoker (KKR) Green's function (GF) method for impurity defects.<sup>19–21</sup> John *et al.* developed a fully relativistic formulation for the magnetic dipolar contribution to  $R$  in the case of ordered paramagnetic systems and did corresponding calculations for transition metals using the LMTO method.<sup>22</sup> Ebert *et al.* developed a similar formulation making use of the KKR Green's function scheme to describe the underlying electronic structure. As could be

demonstrated by an application to the alloy system  $\text{Ag}_x\text{Pt}_{1-x}$ , this allows us in particular to deal with disordered alloys that lack the Bloch translation symmetry.<sup>23</sup> The tremendous flexibility of the Green's function approach has also been exploited by Akai *et al.*, who improved their previous works by taking into account the distortion of the first shell of host Fe atoms around the impurity by means of the technique developed by the Jülich group.<sup>24</sup> In addition, scalar relativistic effects were included properly to treat heavy elements also.<sup>25,26</sup> This approach allowed us to determine the magnetic dipolar contribution to the nuclear spin-lattice relaxation rate  $R_{mag}$  of impurities with atomic number  $Z = 1–57$  and  $72–89$  in bcc Fe using the conventional nonrelativistic formulas for  $R_{mag}$ . The importance of relativistic effects for the spin-lattice relaxation rates in solid transition-metal systems has been demonstrated by Ebert and Akai.<sup>27</sup> These authors did nonrelativistic and relativistic KKR GF calculations for pure transition metals and alloys in the paramagnetic state. In addition they extended the fully relativistic formalism for the magnetic dipolar contribution to  $R$  to deal with magnetic solids as well.

In the following an application as well as an extension of this fully relativistic formalism is presented that accounts for the electric quadrupolar and core polarization contributions  $R_Q$  and  $R_{cp}$ , respectively, to the nuclear spin-lattice relaxation rate in magnetic metals. Because it is based on the spin-polarized and fully relativistic (SPR) KKR Green's function scheme it is applicable for paramagnetic and ferromagnetic systems and also for pure metals, impurities in metals, or disordered alloys. This is demonstrated by an application of this theory to 5d impurities in ferromagnetic bcc Fe, for which the distortion of the surrounded host atoms has been accounted for using the technique developed by the Jülich group.<sup>24</sup> The SPR KKR GF method for impurity systems is described shortly in Sec. II A, and in Sec. II B the formula for the relaxation rate is explained briefly. The formulas of  $R_Q$  and  $R_{cp}$  are derived, in Secs. II C and II D, respectively. In Sec. III the results of applying this theory to calculate the relaxation rate of 5d impurities in bcc Fe are presented and discussed.

## II. THEORETICAL APPROACH

### A. Electronic structure calculations

To describe the underlying electronic structure of the systems investigated their band structure has been calculated by means of the spin-polarized relativistic KKR method. These calculations were based on the relativistic version of the spin density functional theory (SDFT). Within this approach, the single-site Dirac-Kohn-Sham equation

$$\left( -ic\vec{\alpha}\cdot\vec{\nabla} + \frac{c^2}{2}(\beta - I) + V(\vec{r}) \right) \Psi(\vec{r}, E) = E\Psi(\vec{r}, E) \quad (1)$$

has to be solved as a first step. The quantities  $\alpha_i$  and  $\beta$  are the usual Dirac matrices<sup>28</sup> and  $I$  is the  $4 \times 4$  identity matrix. The potential  $V(\vec{r})$  consists of the Hartree term  $V_H(\vec{r})$ , the spin-averaged part  $\bar{V}_{xc}$  of the exchange-correlation potential, and its spin-dependent part,  $V_{spin}$ . This last term is given by

$$V_{spin} = \beta\vec{\sigma}\cdot\frac{dE_{xc}}{d\vec{m}}, \quad (2)$$

where  $\vec{m}$  is the spin magnetization.<sup>29</sup> To set up the exchange-correlation potential, the parametrization given by Vosko, Wilk, and Nusair has been used.<sup>30</sup>

Within the SPR KKR formalism the corresponding Green's function for a pure system (host) is given by<sup>31</sup>

$$G_0(\vec{r}, \vec{r}', E) = \sum_{\Lambda\Lambda'} Z_{\Lambda}(\vec{r}_n, E) \tau_{\Lambda\Lambda'}^{nm} Z_{\Lambda'}^{\times}(\vec{r}'_m, E) - \sum_{\Lambda} Z_{\Lambda}(\vec{r}_{<}, E) J_{\Lambda}^{\times}(\vec{r}_{>}, E) \delta_{nm}, \quad (3)$$

where the functions  $Z_{\Lambda}$  and  $J_{\Lambda}$  are the regular and irregular solutions of Eq. (1), respectively. The index  $\Lambda = (\kappa, \mu)$  represents the spin-orbit  $\kappa$  and magnetic  $\mu$  quantum numbers.  $Z_{\Lambda}$  (and also  $J_{\Lambda}$ ) is a bispinor of the form<sup>28</sup>

$$Z_{\Lambda}(\vec{r}, E) = \begin{pmatrix} g_{\kappa}(r, E) \chi_{\kappa}^{\mu}(\hat{r}) \\ if_{\kappa}(r, E) \chi_{-\kappa}^{\mu}(\hat{r}) \end{pmatrix}, \quad (4)$$

where  $g_{\kappa}$  and  $f_{\kappa}$  are the major and minor radial wave functions, respectively, and  $\chi_{\kappa}^{\mu}$  is the spin-angular function

$$\chi_{\kappa}^{\mu}(\hat{r}) = \sum_{m_s = \pm 1/2} C(l_{\frac{1}{2}} j; \mu - m_s, m_s) Y_l^{\mu - m_s}(\hat{r}) \chi_{m_s}. \quad (5)$$

If  $V_{spin}$  in Eq. (1) is not zero, then  $\kappa$  is not a good quantum number. This applies to ferromagnetic systems and for this case, the former functions must be replaced by

$$Z_{\Lambda}(\vec{r}, E) = \sum_{\Lambda'} Z_{\Lambda'\Lambda}(\vec{r}, E) = \begin{pmatrix} g_{\kappa'\kappa}(r, E) \chi_{\kappa'}^{\mu}(\hat{r}) \\ if_{\kappa'\kappa}(r, E) \chi_{-\kappa'}^{\mu}(\hat{r}) \end{pmatrix}, \quad (6)$$

i.e.,  $Z_{\Lambda}$  has no unique spin-angular character but it is a superposition of various coupled contributions with spin-angular character  $\Lambda'$ .<sup>32</sup> Fortunately it is sufficient to restrict this coupling to  $\Lambda' = (\kappa, \mu)$  and  $(-\kappa - 1, \mu)$ .

Finally, the quantity  $\tau_{\Lambda\Lambda'}^{nm}$  in Eq. (3) is the so-called scattering path operator that represents all multiple scattering

events in the system in a self-consistent way.<sup>31</sup> Accordingly, the indices  $n$  and  $m$  label the various atomic sites in the system.

With the Green's function of the host system set up using Eq. (3), the corresponding Green's function for an impurity system can be set up by application of the Dyson equation. The perturbation caused by the impurity atom  $\alpha$  is then expressed by the perturbed Green's function  $G_{\alpha}(\vec{r}, \vec{r}', E)$  of the atom  $\alpha$ :

$$G_{\alpha}(\vec{r}, \vec{r}', E) = G_0(\vec{r}, \vec{r}', E) + \int d^3 r'' G_0(\vec{r}, \vec{r}'', E) \Delta V(\vec{r}'') G_{\alpha}(\vec{r}'', \vec{r}', E), \quad (7)$$

where  $\Delta V(\vec{r}) = V(\vec{r}) - V_0(\vec{r})$  is the potential perturbation caused by the impurity atom.<sup>25</sup> For the extent of the potential distortion  $\Delta V(\vec{r})$  three different cases have been considered: the impurity atom alone (0 shells), the impurity plus the first shell of nearest-neighbor Fe atoms (1 shell), and the impurity plus the first and the second shells of nearest-neighbor Fe atoms (2 shells). For the three sets of calculations presented below, we have allowed perturbed potentials for every atom of the corresponding clusters, which consist of 1, 9, and 15 atoms, respectively. A geometric relaxation around the impurities has not been allowed. Finally, the angular momentum expansion for the valence band states has been truncated at  $l_{max} = 2$  and the occupied  $f$  levels have been included in the core part (see below).

Apart from the additional complexity introduced by working on a fully relativistic level, the technique to deal with Eq. (7) is just the same as for the scalar relativistic case. For further details we therefore refer to reader to Refs.24 and 33.

### B. Formulas for the total and magnetic nuclear spin-lattice relaxation rate

The nuclear spin-lattice relaxation process in metals is due to magnetic (dipolar) and electric (quadrupolar) interactions between the nuclei and the conduction electrons. The hyperfine Hamiltonian  $\mathcal{H}_{hf}$  that describes, in a relativistically correct form, the interaction between these electrons and a nucleus with spin moment  $\vec{I}$ , gyromagnetic ratio  $\gamma_n$ , and electric quadrupolar moment  $eQ$  is given by

$$\mathcal{H}_{hf} = \mathcal{H}_{mag} + \mathcal{H}_Q, \quad (8)$$

with

$$\mathcal{H}_{mag} = e\vec{\alpha}\cdot\vec{A} = e\gamma_n\hbar\vec{\alpha}\cdot\frac{\vec{I}\times\vec{r}}{r^3}, \quad (9)$$

$$\mathcal{H}_Q = -\sum_{i,j} \frac{e^2 Q}{6I(2I-1)} \left[ \frac{3}{2}(I_i I_j + I_j I_i) - \vec{I}^2 \delta_{ij} \right] \frac{3x_i x_j - r^2 \delta_{ij}}{r^5}. \quad (10)$$

Adopting the spin-temperature approximation the relaxation time  $T_1$  is given as<sup>34</sup>

$$\frac{1}{T_1} = \frac{\sum_{m,m'} W_{m,m'} (E_m - E_{m'})^2}{2 \sum_m E_m^2}, \quad (11)$$

with

$$W_{m,m'} = \frac{2\pi}{\hbar} \sum_{k,k'} | \langle m' k' | \mathcal{H}_{hf} | m k \rangle |^2 k_B T \delta(E_k - E_{m'}) \times \delta(E_{k'} - E_F). \quad (12)$$

For a Zeeman spectrum,  $E_m$  are the nuclear Zeeman energies, and  $W_{m,m'}$  is the total transition probability per unit time for a transition from the nuclear Zeeman level  $|m\rangle$  to the level  $|m'\rangle$ . The state vectors  $|k\rangle$  and  $|k'\rangle$  represent occupied and unoccupied electronic valence levels, respectively. Because there are no cross terms between the magnetic and the electric interactions, the total relaxation rate  $R = (TT_1)^{-1}$  can be divided into two distinct contributions:

$$R = R_{mag} + R_Q = \left( \frac{1}{TT_1} \right)_{mag} + \left( \frac{1}{TT_1} \right)_Q. \quad (13)$$

Ebert *et al.* derived an expression for  $R_{mag}$ , in a Zeeman spectrum, on the basis of the spin-polarized relativistic KKR Green's function scheme<sup>23</sup> using Eqs. (3), (7), (9), (11), and (12):

$$R_{mag} = \frac{4\pi k_B \gamma_n^2 \hbar}{\pi^2} \sum_{\Lambda, \Lambda', \Lambda'', \Lambda'''} \text{Im} \tau_{\Lambda\Lambda'}(E_F) \times \text{Im} \tau_{\Lambda''\Lambda'''}(E_F) I_{\Lambda''\Lambda'}(E_F) I_{\Lambda''\Lambda}^*(E_F), \quad (14)$$

where the matrix elements  $I_{\Lambda\Lambda'}$  are given by

$$I_{\Lambda\Lambda'}(E) = \int d^3\vec{r} \vec{r} Z_{\Lambda}^{\times}(\vec{r}, E) \mathcal{H}_{-}^{el} Z_{\Lambda'}(\vec{r}, E), \quad (15)$$

with

$$\mathcal{H}_{-}^{el} = \frac{e}{2r^3} (\vec{r} \times \vec{\alpha})_{-}. \quad (16)$$

The matrix element  $I_{\Lambda\Lambda'}(E)$  can be split in a conventional way into a product of radial and angular matrix elements  $R_{\kappa\kappa'}(E)$  and  $A_{\Lambda\Lambda'}$ , respectively, of the form<sup>23,28</sup>

$$R_{\kappa\kappa'}(E) = \int [g_{\kappa}(r, E) f_{\kappa'}(r, E) + g_{\kappa'}(r, E) f_{\kappa}(r, E)] dr, \quad (17)$$

$$A_{\kappa\kappa'}^{\mu\mu'} = - \int d\Omega \chi_{\kappa}^{\mu*} \frac{(\vec{r} \times \vec{\sigma})_{-}}{r} \chi_{\kappa'}^{\mu'}. \quad (18)$$

The matrix element  $I_{\Lambda\Lambda'}(E)$  is then finally given as

$$I_{\Lambda\Lambda'}(E) = - \frac{ie}{2} R_{\kappa\kappa'}(E) A_{\kappa\kappa'}^{\mu\mu'}. \quad (19)$$

$R_{mag}$  given in Eq. (14) accounts only for the direct relaxation processes ignoring the electron-electron interaction. Because of the relativistic form of the hyperfine interaction operator [Eq. (9)], it accounts for the conventional nonrelativistic Fermi contact, spin-dipolar, and orbital contributions

to the relaxation rate in one single term. Finally, one should mention that the scattering path operator  $\tau_{\Lambda\Lambda'}(E_F)$  in Eq. (14) is site diagonal (the corresponding index has been suppressed), representing the local electronic properties of the nuclear site. For the applications to be presented here, this will be the site of the impurity atom.

### C. Formula for the electric quadrupolar nuclear spin-lattice relaxation rate

The electric quadrupolar relaxation rate of many nuclei is normally expected to be smaller than the magnetic one, and for this reason, usually not much attention is paid to it. Bloembergen and Rowland pointed out that the electric quadrupolar interaction should be included in the total relaxation rate, because for certain nuclei this rate could be as important as the magnetic rate.<sup>3</sup> Mitchell was one of the first who made numerical approximations of the electric quadrupolar relaxation rate in metals using approximate Bloch wave functions.<sup>4</sup> John *et al.* published a relativistic formula for the electric quadrupolar relaxation rate (and also for the magnetic rate) in cubic metals in the framework of the relativistic LMTO method and applied it to transition metals.<sup>22</sup> Markendorf *et al.* adapted and applied this formula to calculate the electric relaxation rate in hcp transition metals.<sup>12-15</sup> Here, we present a derivation of the relativistic formula of this rate within the SPR KKR GF scheme.

The electric quadrupolar relaxation rate comes from the interaction between the electric quadrupolar moment of the nucleus and the electric field gradient of the charge density of the valence electrons at the nucleus. The Hamiltonian  $\mathcal{H}_Q$  of this interaction can be written in the conventional form:<sup>4,12,34</sup>

$$\mathcal{H}_Q = - \frac{3e^2 Q}{2I(2I-1)r^3} \sum_{m=-2}^2 (-1)^m T_{2m}(\vec{I}) V_{2-m}(\theta, \varphi), \quad (20)$$

with

$$T_{20}(\vec{I}) = \sqrt{\frac{2}{3}} (3I_z^2 - \vec{I}^2), \quad (21)$$

$$T_{2\pm 1}(\vec{I}) = \mp (I_{\pm} I_z + I_z I_{\pm}), \quad (22)$$

$$T_{2\pm 2}(\vec{I}) = I_{\pm}^2, \quad (23)$$

$$V_{2m}(\theta, \varphi) = \sqrt{\frac{2\pi}{15}} Y_2^m(\theta, \varphi). \quad (24)$$

Nuclei with  $I \leq 1/2$  do not have an electric quadrupolar moment  $eQ$ , and hence the rate  $R_Q$  vanishes. Using Eqs. (11), (12), and (20)–(24) we obtain, for a Zeeman spectrum,

$$R_Q = \frac{\pi k_B}{\hbar} \frac{(2I+3)}{5(2I-1)} \left( \frac{3e^2 Q}{4I} \right)^2 (W_1 + 4W_2), \quad (25)$$

with the elements  $W_m$  given by<sup>12</sup>

$$W_m = \sum_{k,k'} \left| \left\langle k' \left| \frac{V_{2m}(\theta, \varphi)}{r^3} \right| k \right\rangle \right|^2 \delta(E_k - E_F) \delta(E_{k'} - E_F). \quad (26)$$

We have derived these elements in the SPR KKR Green's function scheme, by means of Eqs. (3)–(7) and (20)–(24), obtaining

$$W_m = \frac{1}{\pi^2} \sum_{\Lambda, \Lambda', \Lambda'', \Lambda'''} \text{Im} \tau_{\Lambda\Lambda'}(E_F) \times \text{Im} \tau_{\Lambda''\Lambda'''}(E_F) J_{\Lambda'''\Lambda}(E_F) J_{\Lambda''\Lambda'}^*(E_F), \quad (27)$$

where the corresponding matrix elements  $J_{\Lambda\Lambda'}$  are given by

$$J_{\Lambda\Lambda'}(E) = \int d^3\vec{r} Z_{\Lambda}^{\times}(\vec{r}, E) \frac{V_{2m}(\theta, \varphi)}{r^3} Z_{\Lambda'}(\vec{r}, E) = S_{\kappa\kappa'}(E) B_{\kappa\kappa'}^{\mu\mu'm}, \quad (28)$$

with the radial and the angular parts, respectively, equal to

$$S_{\kappa\kappa'} = \int (g_{\kappa} g_{\kappa'} + f_{\kappa} f_{\kappa'}) \frac{dr}{r}, \quad (29)$$

$$B_{\kappa\kappa'}^{\mu\mu'm} = \int d\Omega \chi_{\kappa}^{\mu*} V_{2m}(\theta, \varphi) \chi_{\kappa'}^{\mu'}. \quad (30)$$

In Eq. (29) we have suppressed the arguments  $r$  and  $E$ . The angular part  $B_{\kappa\kappa'}^{\mu\mu'm}$  can be further expressed in terms of Clebsch-Gordan coefficients:

$$B_{\kappa\kappa'}^{\mu\mu'm} = \sqrt{\frac{2l'+1}{6(2l+1)}} C(2l'l; 000) [C(l\frac{1}{2}j; \mu - \frac{1}{2}\frac{1}{2}\mu) \times C(l'\frac{1}{2}j'; \mu' - \frac{1}{2}\frac{1}{2}\mu') C(2l'l; m\mu' - \frac{1}{2}\mu - \frac{1}{2}) + C(l\frac{1}{2}j; \mu + \frac{1}{2} - \frac{1}{2}\mu) C(l'\frac{1}{2}j'; \mu' + \frac{1}{2} - \frac{1}{2}\mu') \times C(2l'l; m\mu' + \frac{1}{2}\mu + \frac{1}{2})]. \quad (31)$$

At this point it is interesting to compare the magnetic and the electric quadrupolar relaxation rates for a Zeeman spectrum. Using Eqs. (14) and (25), and the values of  $g_n$  ( $g_n \mu_n = \gamma_n \hbar$ ),  $I$ , and  $Q$  for the 5d elements in Table I, and taking into account the dimensions of the matrix elements  $I_{\Lambda\Lambda'}(E_F)$  and  $J_{\Lambda\Lambda'}(E_F)$ , then it is possible to estimate the ratio  $r$  between these two relaxation rates as

$$r = \frac{R_Q}{R_{mag}} \sim \left( \frac{eQ}{a_0 g_n \mu_n I} \right)^2 \sim 10^{-3} - 10^{-4}, \quad (32)$$

where  $a_0$  is the Bohr radius. In this estimation the crude supposition has been made that the dimensionless matrix elements of both relaxation mechanisms are of the same order of magnitude. In contrast to that assumption, the dimensionless matrix elements  $I_{\Lambda\Lambda'}(E_F)$  of  $R_{mag}$  are found, in our calculations of 5d elements, to be about  $10-10^{-4}$  times those of  $R_Q$ ,  $J_{\Lambda\Lambda'}(E_F)$ . This means that for certain cases  $R_Q$  could be bigger than  $R_{mag}$  or at least, not negligible with respect to the magnetic rate.

TABLE I. Nuclear spin moment, nuclear  $g$  factor  $g_n$  (a dimensionless quantity) and electric quadrupolar constant  $Q$  in barns ( $eQ$  is the electric quadrupolar moment) of the two most abundants nuclei of the 5d atoms with a nonvanishing nuclear moment. The number of nucleons of the nuclei is indicated. For Hf, Re, Ir, and Hg there are two isotopes.

	Lu	Hf	Ta	W	Re		
	175	177	179	181	183	185	187
$I$	7/2	7/2	9/2	7/2	1/2	5/2	5/2
$g_n$	0.639	0.227	-0.142	0.677	0.236	1.275	1.288
$Q$	5.68	4.50	5.10	3.44	0	2.33	2.22
	Os	Ir	Pt	Au	Hg		
	189	191	193	195	197	199	201
$I$	3/2	3/2	3/2	1/2	3/2	1/2	3/2
$g_n$	0.488	0.097	0.107	1.219	0.098	1.012	-0.373
$Q$	0.80	0.78	0.70	0	0.59	0	0.42

#### D. Formula for the core polarization relaxation rate

Yafet and Jaccarino suggested that the core polarization (CP) mechanism should contribute to the magnetic relaxation rate just as it does for the Knight shift.<sup>7</sup> These authors derived an expression for the core polarization relaxation rate  $R_{cp}$  and made corresponding estimations for V, Nb, and Pt. Since the exchange energies responsible for the CP mechanism are small compared with the transition energies, they did a first-order perturbation type calculation for the CP rate. This approach led to a Korringa-like relation between the CP Knight shift and the CP relaxation rate, with the corresponding Korringa ratio depending on the relative weight of the various symmetry-resolved orbitals with  $d$  character. Hence, using reasonable estimations for the hyperfine fields to calculate that ratio, they calculated the CP rate and obtained values of 1.65, 3.74, and 54.2 (s K)<sup>-1</sup> for V, Nb, and Pt, respectively.

Asada *et al.* have calculated  $R_{cp}$  of some cubic transition metals using LMTO band structure calculations.<sup>9</sup> To calculate the CP rate they used the approximate formula suggested by Yafet and Jaccarino. In this formula, the CP rate is proportional to  $\mathcal{H}_{cp}^2$ , the square of the nonrelativistic core polarization hyperfine coupling constant, defined as

$$\mathcal{H}_{cp} = \frac{8\pi}{3} \mu_B \sum_s \frac{\rho_{s\uparrow}(0) - \rho_{s\downarrow}(0)}{m_d}, \quad (33)$$

where the sum runs over all  $s$ -like core electrons with density  $\rho_{sm_s}(\vec{r})$  and spin character  $m_s$ , and  $m_d$  is the number of unpaired  $d$  electrons. They found values for  $R_{cp}$  between 0.076 and 0.0007 (s K)<sup>-1</sup> for V, Nb, Mo, Rh, Pd, Ag, and Cu. For V and Nb, they obtained 0.076 and 0.068 (s K)<sup>-1</sup>, respectively. Asada and Terakura did also scalar relativistic LMTO band structure calculations for hcp transition metals.<sup>10</sup> They used the same approach to calculate  $R_{cp}$  and obtained values smaller than 0.12 (s K)<sup>-1</sup> for Sc, Ti, Y, Zr, and Tc. Akai calculated the spin-nuclear relaxation rate of impurities in bcc Fe by means of a KKR GF method for impurity systems.<sup>25,26</sup> In particular, he considered a cluster composed by the impurity atom and the first nearest-eight-



neighbor Fe atoms. He also included the relativistic effects, but only in the scalar relativistic approximation, neglecting the spin-orbit coupling, and applied the same approach to calculate  $R_{cp}$  as Asada *et al.*<sup>9</sup> Finally, Markendorf *et al.* did not recalculate  $R_{cp}$ ,<sup>14</sup> but used the values obtained by Asada and Terakura.<sup>10</sup>

All these authors used nonrelativistic expressions to calculate  $R_{cp}$ . In contrast to this, we have formulated a consistent and relativistic formula for  $R_{cp}$ , using a scheme similar to that of Yafet and Jaccarino.<sup>7</sup> For this purpose, only the contribution of the  $s$ -like core electrons to the core polarization effect has been considered. This is the most important contribution because the hyperfine matrix element is the largest for  $s$ -like core electrons.

Treating the exchange interaction as a first-order perturbation, an unoccupied one-electron orbital  $|\Psi_k\rangle$  of an atom, mixed with the  $s$  orbitals of the core electrons of that atom, has the following form:

$$|\Psi_k\rangle = |\Psi_k^0\rangle + \sum_{ns} C_{ns,k} |\Psi_{ns}^0\rangle = |\Psi_k^0\rangle + A |\Psi_k^0\rangle, \quad (34)$$

with

$$C_{ns,k} = \frac{\langle \Psi_{ns}^0 | \Delta v_{xc} | \Psi_k^0 \rangle}{E_F^0 - E_{ns}^0}. \quad (35)$$

The sum runs over the principal quantum numbers  $n$  of the  $s$ -like core orbitals of the atom, including the spin up and down orbitals for each value of  $n$ , and the index 0 denotes the unperturbed orbitals. For the magnetic rate one has, then

$$R_{mag} = 4\pi k_B \gamma_n^2 \hbar \sum_{k,k'} |\langle \Psi_{k'} | H_-^{el} | \Psi_k^0 \rangle|^2 \delta(E_k - E_F) \times \delta(E_{k'} - E_F). \quad (36)$$

The squared quantity of Eq. (36) is given by

$$|\langle \Psi_{k'} | H_-^{el} | \Psi_k^0 \rangle|^2 = |\langle \Psi_{k'}^0 | H_-^{el} | \Psi_k^0 \rangle|^2 + |\langle \Psi_{k'}^0 | A^\dagger H_-^{el} | \Psi_k^0 \rangle|^2, \quad (37)$$

where the cross terms do not appear for cubic systems.<sup>7</sup>

The first and the second terms are leading to  $R_{mag}$  and  $R_{cp}$ , respectively. The second term can be further developed and the core polarization rate has, then, the expression

$$R_{cp} = \frac{4\pi k_B \gamma_n^2 \hbar}{\pi^2} \sum_{\Lambda, \Lambda', \Lambda'', \Lambda'''} \text{Im} \tau_{\Lambda \Lambda'}(E_F) \times \text{Im} \tau_{\Lambda'' \Lambda'''}(E_F) M_{\Lambda \Lambda'}(E_F) M_{\Lambda'' \Lambda'''}^*(E_F). \quad (38)$$

Here the matrix element  $M_{\Lambda \Lambda'}$  is

$$M_{\Lambda \Lambda'}(E) = \int d^3 r Z_{\Lambda}^{\times}(\vec{r}, E) A^{\times} H_-^{el} Z_{\Lambda'}(\vec{r}, E) = \sum_{n=1}^N \sum_{\mu_s = -1/2}^{+1/2} \times V_{\kappa \kappa_s n \mu_s}(E) \delta_{\mu \mu_s} \delta_{\kappa \kappa_s} R_{\kappa_s n \mu_s \kappa'}(E) A_{\kappa_s \kappa'}^{\mu_s \mu'}, \quad (39)$$

where  $\Lambda_s$  indicates the  $s$ -like core levels, which have  $l=0$  and hence  $\Lambda_s = (\kappa_s, \mu_s) = (-1, \pm 1/2)$ ,  $N$  is the number of occupied  $s$ -like core shells, and the other quantities are defined by

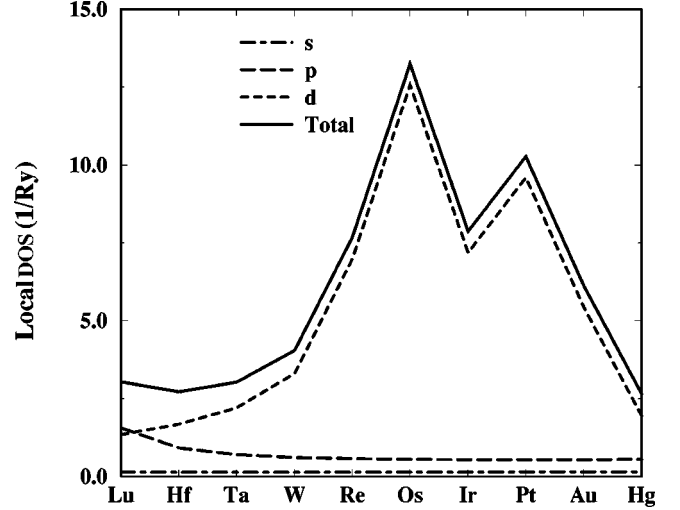


FIG. 1. Total,  $s$ ,  $p$ , and  $d$  local density of states at the Fermi energy of the  $5d$  atoms in bcc Fe, obtained by calculations for a 0-shell cluster.

$$V_{\kappa n \kappa_s \mu_s}(E) = \int (g_{\kappa} g_{n \kappa_s \mu_s} + f_{\kappa} f_{n \kappa_s \mu_s}) \Delta v_{xc} r^2 dr, \quad (40)$$

$$R_{n \kappa_s \mu_s \kappa'}(E) = \int (g_{n \kappa_s \mu_s} f_{\kappa'} + g_{\kappa'} f_{n \kappa_s \mu_s}) dr. \quad (41)$$

The angular matrix element  $A_{\kappa_s \kappa'}^{\mu_s \mu'}$  is the same as that given in Eq. (18). The magnitude  $\Delta v_{xc}$  is the change of the exchange-correlation energy due to a difference of only one electron between the electrons with spin up and down, or in other words, to the magnetization due to only one electron.<sup>35</sup>

Finally, it should be noted that Götz and Winter<sup>36</sup> developed a scheme to account for the influence of electron-electron interactions on the nuclear spin-lattice relaxation rate by solving a corresponding Bethe-Salpeter equation for the dynamical spin susceptibility. However, this approach did not include the core electrons and was formulated in a scalar relativistic way. A corresponding relativistic extension that include the core electrons should lead to similar results as those given here.

### III. APPLICATION TO $5d$ IMPURITIES IN bcc Fe: RESULTS AND DISCUSSION

In the following the results of the calculations of the various contributions to the spin-lattice relaxation rate of  $5d$  impurities in bcc Fe will be presented. To facilitate comparison of the results for the various elements, the rates will, in general, be given in an isotope-independent way. For the magnetic rates  $R_{mag}$  and  $R_{cp}$  this means, for example, that they will be normalized by the factor  $1/g_n^2$ .

In Figs. 1 and 2 we present the local density of states (DOS) at the Fermi energy of the  $5d$  impurities and their magnetic reduced relaxation rates  $R_{mag}/g_n^2$  obtained in our calculations. Both figures refer to calculations for a 0-shell cluster, i.e., only the impurity atom has been embedded self-consistently into the bcc Fe host lattice. Comparing these figures we can see that the trends of the different components of  $R_{mag}/g_n^2$  ( $s$ ,  $p$ , and  $d$ ) reflect, in general, the trends of the

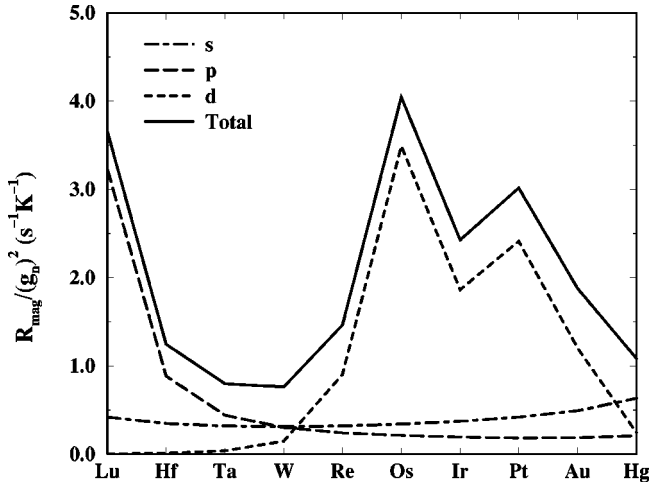


FIG. 2. Magnetic reduced relaxation rates  $R_{mag}/g_n^2$  of the  $5d$  atoms in bcc Fe, obtained by calculations for a 0-shell cluster.

corresponding components of the local DOS. The  $s$  component of  $R_{mag}/g_n^2$  (and also of the local DOS) increases slowly along the  $5d$  series when increasing the atomic number and it is very small. On the other hand, the  $p$  component decreases rapidly along the  $5d$  series, as the  $p$  DOS, while the  $d$  component follows the more complicated behavior of the local  $d$  DOS.

In contrast to this behavior, one notes that the sequence of the components of the local DOS with respect to their magnitude differs from that of the components of the magnetic reduced rate. Although the local  $d$  DOS is bigger than the  $p$  DOS (except for Lu, where both are similar) the  $d$  component of  $R_{mag}/g_n^2$  is only bigger than the  $p$  component for the late  $5d$  transition metals.

To understand this fact we have to take into account the variation of the corresponding radial matrix elements  $R_{\kappa\kappa'}(E_F)$  [see Eq. (17)] with the atomic number. These are represented in Fig. 3 by the so-called hyperfine fields  $B_{hf,\kappa}$ . These fields are proportional to the normalized radial matrix elements  $\bar{R}_{\kappa\kappa}(E_F)$  that are obtained from Eq. (17) but with the wave functions normalized to 1 within the atomic cell. In

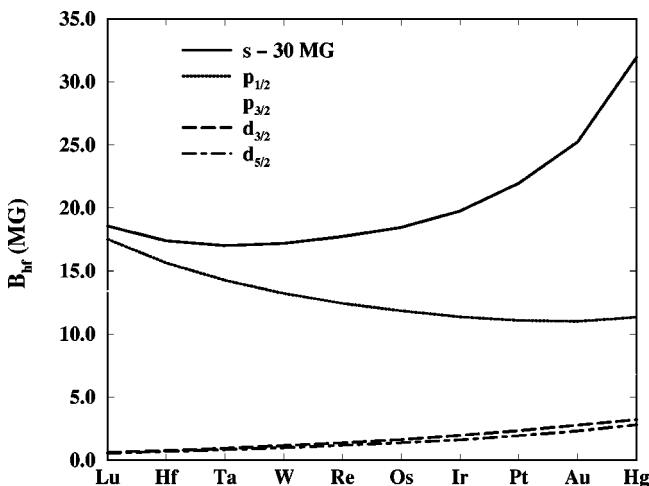


FIG. 3. Hyperfine fields for  $s_{1/2}$ ,  $p_{1/2}$ ,  $p_{3/2}$ ,  $d_{3/2}$ , and  $d_{5/2}$  of the  $5d$  atoms in bcc Fe, obtained by calculations for a 0-shell cluster. The hyperfine field for  $s_{1/2}$  has been shifted down by 30 MG.

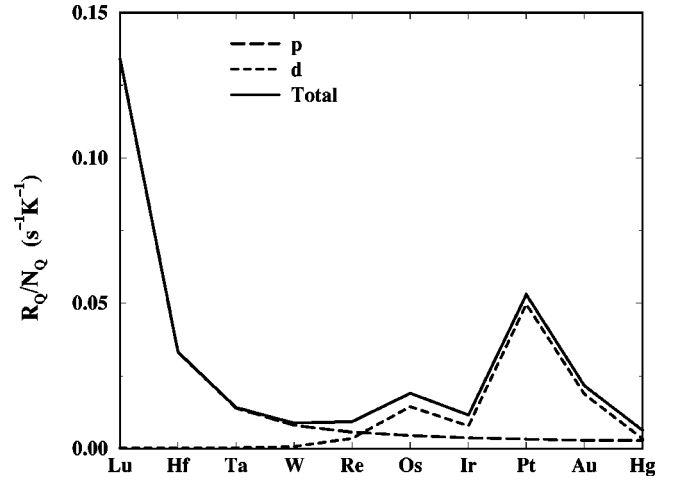


FIG. 4. Isotope-independent electric quadrupolar relaxation rates  $R_Q/N_Q$  of the  $5d$  atoms in bcc Fe, obtained by calculations for a 0-shell cluster.

contrast to the paramagnetic case,<sup>23,27</sup>  $B_{hf,\kappa}$  depends, for the magnetic case, also on the magnetic quantum number  $\mu$ . For the discussion that follows below, however, it is sufficient to fix  $\mu$  to an arbitrary value ( $\mu = +1/2$  has been chosen here). In addition, only the fields diagonal in  $\kappa$  are considered and only the  $l$  dependence is of importance for our considerations.<sup>27,37</sup>

The results shown in Fig. 3 allow us to understand why the trends of the components of the reduced magnetic rate do not reflect those of the components of the local DOS: the hyperfine fields modulate the variation of the local  $s$ ,  $p$ , and  $d$  DOS with the atomic number. Although  $B_{hf,s}$  is large, the  $s$  component of the reduced magnetic rate is quite small because the local  $s$  DOS is very small.  $B_{hf,p}$  and  $n_p$  decrease rapidly when increasing the atomic number, and hence also the  $p$  reduced magnetic rate decreases. It can be seen in Fig. 3 that  $B_{hf,s}$  is between 3 and 5 times bigger than  $B_{hf,p}$  for the  $5d$  transition metals, but at the same time is the local  $s$  DOS between 12 and 4 times smaller than the local  $p$  DOS. These two facts explain that the  $p$  rate is much bigger than the  $s$  rate at the beginning of the  $5d$  series and that the  $s$  rate is similar or even bigger than the  $p$  rate for the rest of the  $5d$  series.  $B_{hf,d}$  increases with the atomic number and rises from 0.6 to 3.2 MG. This hyperfine field is between 80 and 20 times smaller than  $B_{hf,s}$ , but on the other hand, the  $d$  DOS is between 10 and 100 times bigger than the  $s$  DOS. This explains why the  $s$  rate is bigger than the  $d$  rate for the first four atoms but much smaller for the other atoms.

In Fig. 4 we show the isotope-independent electric quadrupolar relaxation rate  $R_Q/N_Q$  of  $5d$  impurities in bcc Fe obtained by calculations for the 0-shell cluster. The normalization factor  $N_Q$  contains all the quantities of  $R_Q$  in Eq. (25) that depend on the type of isotope and is given by

$$N_Q = \left(\frac{Q}{I}\right)^2 \frac{2I+3}{2I-1}. \quad (42)$$

Application of this normalization factor allows us to demonstrate the influence of the components of the local DOS on the electric quadrupolar rate. However, one has to keep in mind that in the experiments the measured relaxation rate

includes the electric quadrupolar rate  $R_Q$  and that the rate  $R_Q$  of the nuclei with  $I \leq 1/2$  is zero.

The  $s$  component does not appear because it is zero, due to the selection rules emerging from Eq. (31). Similar to  $R_{mag}/g_n^2$ , the components of  $R_Q/N_Q$  follow also the trends of the corresponding components of the local DOS. As for the magnetic rate, the  $p$  component is the most important component for the first four atoms of the  $5d$  series, while for the rest the  $d$  component dominates. The  $p$  component of  $R_Q/N_Q$  decreases rapidly when increasing the atomic number, following the  $p$  DOS. Although the  $d$  DOS is always bigger than the  $p$  DOS, except in Lu, the  $d$  component of  $R_Q/N_Q$  does not exceed the  $p$  component in a corresponding way. For instance, the  $d$  DOS is between 11 and 25 times larger than the  $p$  DOS for Re–Au, but the  $d$  component of  $R_Q/N_Q$  is only between 0.6 and 15 times the  $p$  component. This is explained again qualitatively by taking into account that every component of the electric quadrupolar rate is not only proportional to the square of the component of the DOS but also to the square of the radial integral  $S_{\kappa\kappa}$  given in Eq. (29). As one can conclude from the nonrelativistic counterparts of the magnetic hyperfine fields  $B_{hf,\kappa}$  for non- $s$  electrons ( $l \neq 0$ ),<sup>27</sup> these vary in parallel with  $S_{\kappa\kappa}$  along the  $5d$  transition series. In summary, one finds at the beginning of the  $5d$  series a relatively high  $p$  DOS at  $E_F$  that leads to a dominating and large contribution to  $R_Q/N_Q$ .

There could be an interaction between occupied (unoccupied)  $p$ ,  $d$ , and unoccupied (occupied)  $f$  valence levels of the  $5d$  impurity. However, for these types of impurities the  $4f$  shell is a closed shell and for that reason the  $4f$  electrons of the  $5d$  impurities have been included as core electrons. On the other hand, the unoccupied  $f$  valence levels of these impurities are expected to contribute to the density of states at the Fermi level only in a negligible way. As a consequence their contribution to the various relaxation rates have been ignored. Among others, this is justified by comparing our results with those of Akai.<sup>25</sup>

To discuss the trend of the total relaxation rate  $R$  along the  $5d$  series, one has to combine the magnetic dipolar and electric quadrupolar contribution. The latter will be represented by the quantity  $R_Q/g_n^2$  that depends now on the specific isotope. The corresponding values for  $g_n$ ,  $I$ , and  $Q$  are given in Table I. The resulting rates  $R_{mag}/g_n^2$  and  $R_Q/g_n^2$  obtained for 0-shell clusters are shown in Fig. 5. One notes that the magnetic reduced rate  $R_{mag}/g_n^2$  is in general bigger than the electric quadrupolar one and that the  $p$  component of the total reduced rate is the most important component for the first four atoms of the  $5d$  series while the rest of the series is dominated by the  $d$  contribution.

The core polarization rate is not shown separately in Fig. 5 because it is very small. According to our calculations  $R_{cp}/g_n^2$  is about  $10^{-6}$  (s K)<sup>-1</sup> for all the  $5d$  elements. This is to be compared with the calculations of Akai that gave  $R_{cp}/g_n^2$  only a few percent of the total rate for all the nuclei studied.<sup>25,26</sup> In particular, for the  $5d$  series its value is between  $10^{-3}$  (s K<sup>-1</sup>) and  $10^{-4}$  (s K)<sup>-1</sup>.<sup>38</sup> Because the  $p_{1/2}$  core orbitals have a small  $s$ -like minor component there should be an analogous contribution to the core polarization rate as the one considered here. However, taking into account the results for the  $s$ -like core orbitals, the  $p_{1/2}$  contri-

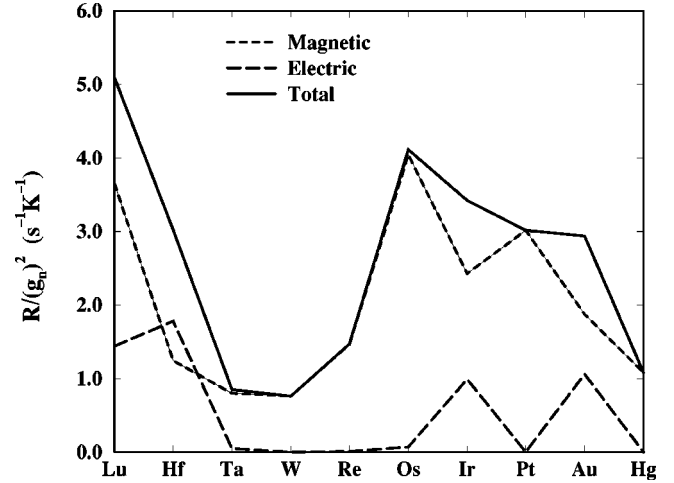


FIG. 5. Total, magnetic, and electric quadrupolar reduced relaxation rates of the  $5d$  atoms in bcc Fe obtained in calculations of the 0-shell cluster.

bution to the core polarization rate will be even smaller. This means that the formulation for the CP contribution to  $R_{mag}$  presented here leads to a much smaller CP rate than the conventional approach and for that reason it can safely be neglected. Thus, it can be seen from Fig. 5 that the main contribution to the total reduced rate comes from the magnetic interaction, except for Hf. Besides,  $R_Q/g_n^2$  is not negligible respect to  $R_{mag}/g_n^2$  for Lu and Hf, because their big values of  $Q$ , and for Ir, and Au, because their small values of  $g_n^2$ . As a consequence, the electric quadrupolar reduced relaxation rate of Lu, Hf, Ir, and Au relatively amounts to be 28%, 59%, 29%, and 36% of the total reduced rate.

The influence of the cluster size on the local DOS and the total reduced rate  $R/g_n^2$  is considered in Figs. 6 and 7, respectively. In line with the variation of the DOS, the total rate decreases in the first part of the  $5d$  series when allowing perturbed potentials also on the first neighboring shell. In the second part of the series, it increases. The local DOS of the 1-shell cluster is not very different of that of the 2-shell clusters and therefore also the corresponding total rates scarcely differ.

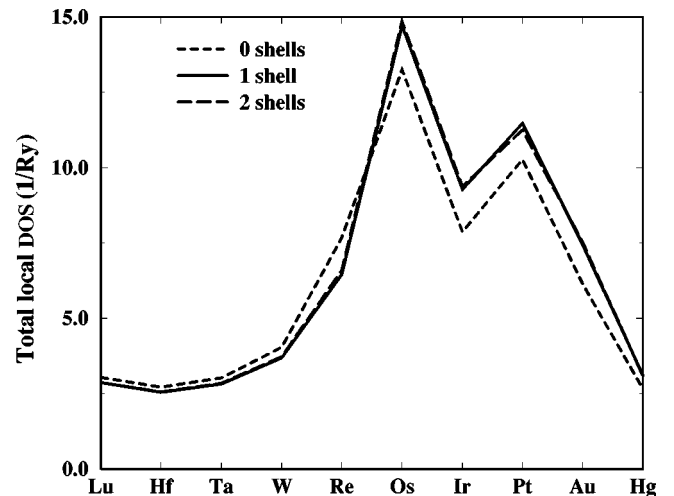


FIG. 6. Total density of states at the Fermi energy of the  $5d$  atoms in bcc Fe, obtained in calculations of the 0-, 1-, and 2-shell clusters.

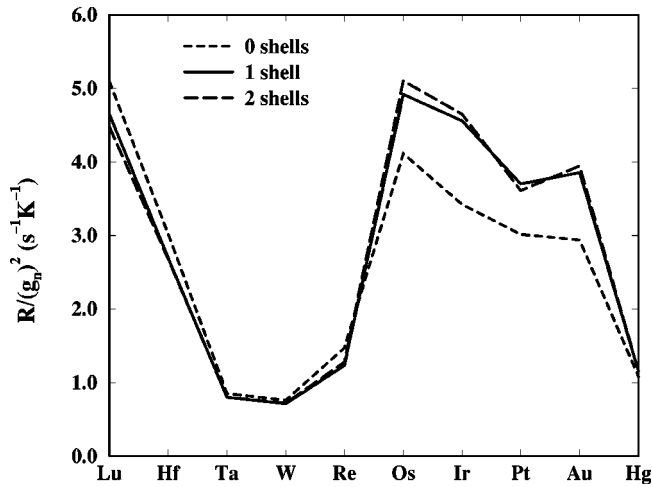


FIG. 7. Total reduced relaxation rates  $R/g_n^2$  of the  $5d$  atoms in bcc Fe, obtained in calculations of 0-, 1-, and 2-shell clusters.

Our results of  $R_{mag}/g_n^2$  for the 1-shell cluster agree very well with the results obtained by Akai, for the same cluster size,<sup>25,26</sup> as can be seen in Fig. 8. However, there are some differences in the second part of the  $5d$  series that have to be ascribed to the inclusion of the spin-orbit coupling interaction, neglected within the calculations of Akai. Hence, one has to conclude from Fig. 8 that the influence of the spin-orbit on the relaxation rate is surprisingly small. As a consequence, the explanation for the variation of the magnetic relaxation rate with the atomic number given by Akai<sup>20,25</sup> can also be applied to the present calculations: There is a competition between two factors. The Fermi contact interaction [one of the main interactions inherently included in the relativistic Hamiltonian, Eq. (9)] increases with the impurity valence, which increases with the atomic number in the  $5d$  series, and hence also the magnetic relaxation rate. On the other hand, the impurity potential gets deeper as the impurity valence increases. The deeper potential pulls down the peaks of the local DOS associated with the antibonding states of both spin directions until they pass the Fermi level. As a

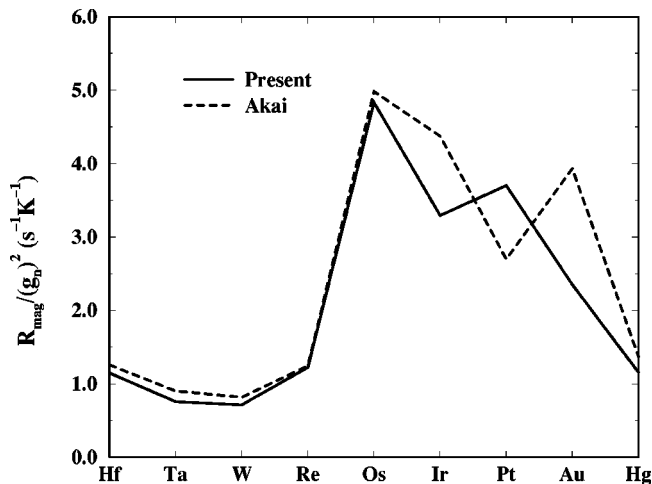


FIG. 8. Magnetic reduced relaxation rates  $R_{mag}/g_n^2$  of the  $5d$  atoms in bcc Fe, obtained in the present calculations of the 1-shell cluster and by Akai (Refs. 25 and 26).

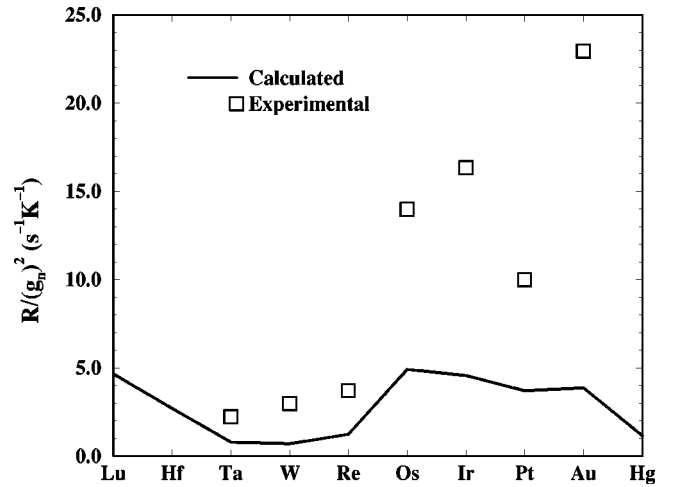


FIG. 9. Experimental (Ref. 39) and calculated total reduced relaxation rates  $R/g_n^2$  of the  $5d$  atoms in bcc Fe, obtained in calculations of 1-shell clusters.

consequence, the local DOS at the Fermi energy finally decreases, and hence the magnetic relaxation rate also decreases.

Funk *et al.* have recently given a critical review for the nuclear spin-lattice relaxation rate of transition impurities in Fe,<sup>39</sup> and have compared them with the results of Akai *et al.*<sup>19–21,25,26</sup> In Fig. 9 we compare the calculated reduced relaxation rates with the experimental values quoted by these authors. It can be seen that the calculated rates reproduce the trend of the experimental rates of the  $5d$  impurities in Fe quite well, but they are about 3–5 times smaller than the experimental ones. Akai *et al.* suggested that the discrepancies between theoretical and experimental relaxation rates of transition impurities in Fe are caused by geometric lattice relaxation around the impurities because the discrepancies increase with the size of the impurity.<sup>19–21,25,26</sup> However, Funk *et al.* have indicated that in the case of Fe seen as an impurity in the Fe host lattice the discrepancy is similar to those for the other  $3d$  impurities in Fe.<sup>39</sup> Furthermore, the static hyperfine fields calculated by Akai<sup>19,20,26</sup> and also by Ebert *et al.*<sup>40</sup> are in a reasonable agreement with the experimental fields. All this suggests that there is a relaxation mechanism that it is not taken into account in the calculations. In particular, the theory does not deal with excitations of the host lattice (phonons and magnons) and Funk *et al.* have shown that the neglect of the Weger mechanism,<sup>41</sup> i.e., the excitation of virtual magnons by relaxing nuclei, leads to a systematic underestimation of the relaxation rates of transition impurities in Fe.<sup>39,42,43</sup> They added phenomenological estimates for the virtual magnon contribution by Masuda *et al.*<sup>16,44</sup> to the results of Akai for transition impurities in Fe and found a better agreement with the experimental results.<sup>42,43,39</sup> The agreement between the calculated rates by Akai *et al.* and the experimental rates decreases with the size of the impurity and for  $3d$  impurities the agreement is quite satisfying. This is in line with the work of Funk *et al.*,<sup>39</sup> who demonstrated that, in general, the magnon contribution increases with the size of the impurity.

Another effect influencing the relaxation rate that has not been accounted for in our calculations nor in the previous ones are the domain wall effects. For ferromagnetic systems



the relaxation rates depend strongly on the intensity of the applied magnetic field, but converge to a value at high fields, the so-called high-field limit value. The calculated rates correspond to this high-field limit. The low-field relaxation rates often exceed the high-field rates by an order of magnitude. Several authors suggested that this field dependence at low fields and also the difference between low- and high-field rates is caused by the fact that the nuclei in the neighborhood of a domain wall relax much faster than those within a domain. Klein claimed that this mechanism should not be able to explain, for instance, a field dependence within up to 0.5 T for Co in Fe (Ref. 45) or 1.2 T for Fe in Fe (Ref. 39) as an effect of domain walls.<sup>45</sup> Besides, according to some experiments, the relaxation rate in a single domain is also field dependent at low fields.<sup>45</sup>

#### IV. CONCLUSIONS

We have derived fully relativistic expressions for the electric quadrupolar and the core polarization nuclear spin-lattice relaxation rates in the framework of the SPR KKR GF method. These expressions are valid for paramagnetic as well as magnetically ordered systems. We have done corresponding fully relativistic and spin-polarized KKR GF calculations for the angular momentum resolved components of the total rate  $R$ , the magnetic rate  $R_{mag}$ , the electric quadrupolar rate  $R_Q$ , and the core polarization rate  $R_{cp}$  of  $5d$  impurities in bcc Fe.

We have found in our calculations that the magnetic relaxation rate is bigger than the electric quadrupolar rate, as it was found in previous nonrelativistic investigations, except for Hf. In addition, the electric quadrupolar relaxation rate

turned out to be non-negligible with respect to the magnetic one in Lu, Hf, Ir, and Au. The core polarization reduced relaxation rate  $R_{cp}/g_n^2$  was found to be very small, of the order of  $10^{-6}$  (s K)<sup>-1</sup>. Again, previous work of other authors also indicated that this rate is very small.<sup>25,26</sup> The trend of the angular momentum resolved ( $s$ ,  $p$ , and  $d$ ) parts of the magnetic reduced rate  $R_{mag}/g_n^2$  follows the trend of the corresponding local angular DOS at  $E_F$ . The  $p$  conduction electrons were found to be the main source for the electric quadrupolar rate and the trend of the  $p$  component of this rate follows again the trend of the local  $p$  DOS. Potential relaxation of the first shell of neighboring Fe atoms has a non-negligible influence on the relaxation rates. On the other hand, inclusion of the potential relaxation for the second shell, in addition to the first shell, leads only to marginal changes. The agreement with previous calculations by Akai, done in a scalar relativistic way, is very good,<sup>25,26</sup> with the differences ascribed to the effect of the spin-orbit coupling interaction. The calculated total rates are about 3–5 times smaller than the experimental ones, mainly due to the neglect of the contribution of the magnons in the theory.<sup>39</sup>

#### ACKNOWLEDGMENTS

This work was funded by the DFG (Deutsche Forschungsgemeinschaft) within the program *Theorie relativistischer Effekte in der Chemie und Physik schwerer Elemente*. I.C. wishes to thank the European Commission for a grant of the TMR network *Ab-initio Calculations of Magnetic Properties of Surfaces, Interfaces and Multilayers* in the Fourth Program for Research and Technological Development and to thank all the members of H.E.'s group for their hospitality.

- 
- <sup>1</sup>W. Heitler and E. Teller, Proc. R. Soc. London, Ser. A **155**, 637 (1936).  
<sup>2</sup>J. Koringa, Physica (Amsterdam) **16**, 601 (1950).  
<sup>3</sup>N. Bloembergen and T. J. Rowland, Acta Metall. **1**, 731 (1953).  
<sup>4</sup>A. H. Mitchell, J. Chem. Phys. **26**, 1714 (1957).  
<sup>5</sup>Y. Obata, J. Phys. Soc. Jpn. **18**, 1020 (1963).  
<sup>6</sup>Y. Obata, J. Phys. Soc. Jpn. **19**, 2348 (1964).  
<sup>7</sup>Y. Yafet and V. Jaccarino, Phys. Rev. **133**, 1630 (1964).  
<sup>8</sup>A. Narath, Phys. Rev. **163**, 232 (1967).  
<sup>9</sup>T. Asada, K. Terakura, and T. Jarlborg, J. Phys. F: Met. Phys. **11**, 1847 (1981).  
<sup>10</sup>T. Asada and K. Terakura, J. Phys. F: Met. Phys. **12**, 1387 (1982).  
<sup>11</sup>T. Asada and K. Terakura, J. Phys. F: Met. Phys. **13**, 799 (1983).  
<sup>12</sup>R. Markendorf, Ph.D. thesis, University of Dresden, 1991.  
<sup>13</sup>R. Markendorf, Z. Naturforsch., A: Phys. Sci. **49**, 395 (1994).  
<sup>14</sup>R. Markendorf, C. Schober, and W. John, J. Phys.: Condens. Matter **6**, 3965 (1994).  
<sup>15</sup>R. Markendorf and C. Schober, J. Phys.: Condens. Matter **7**, 4561 (1995).  
<sup>16</sup>Y. Masuda, T. Hioki, and M. Kontani, Int. J. Magn. **6**, 143 (1974).  
<sup>17</sup>T. Moriya, J. Phys. Soc. Jpn. **19**, 681 (1964).  
<sup>18</sup>J. Kanamori, H. K. Yoshida, and K. Terakura, Hyperfine Interact. **9**, 363 (1981).  
<sup>19</sup>M. Akai, H. Akai, and J. Kanomori, J. Phys. Soc. Jpn. **54**, 4246 (1985).  
<sup>20</sup>H. Akai, M. Akai, and J. Kanamori, J. Phys. Soc. Jpn. **54**, 4257 (1985).  
<sup>21</sup>M. Akai, H. Akai, and J. Kanamori, J. Phys. Soc. Jpn. **56**, 1064 (1987).  
<sup>22</sup>W. John, V. V. Nemoshkalenko, and V. N. Antonov, in *Proceedings of the 13th International Symposium on Electronic Structure of Metals and Alloys* (Johnsbach, 1983), p. 236.  
<sup>23</sup>H. Ebert, P. Weinberger, and J. Voitländer, Phys. Rev. B **31**, 7566 (1985).  
<sup>24</sup>P. J. Braspenning, R. Zeller, A. Lodder, and P. H. Dederichs, Phys. Rev. B **29**, 703 (1984).  
<sup>25</sup>H. Akai, Hyperfine Interact. **43**, 255 (1988).  
<sup>26</sup>H. Akai, M. Akai, S. Blügel, B. Drittler, H. Ebert, K. Terakura, R. Zeller, and P. H. Dederichs, Prog. Theor. Phys. Suppl. **101**, 11 (1990).  
<sup>27</sup>H. Ebert and H. Akai, Hyperfine Interact. **78**, 361 (1993).  
<sup>28</sup>M. E. Rose, *Relativistic Electron Theory* (Wiley, New York, 1961).  
<sup>29</sup>A. H. MacDonald and S. H. Vosko, J. Phys. C **12**, 2977 (1979).  
<sup>30</sup>S. H. Vosko, L. Wilk, and M. Nusair, Can. J. Phys. **58**, 1200 (1980).  
<sup>31</sup>P. Weinberger, *Electron Scattering Theory for Ordered and Disordered Matter* (Oxford University Press, Oxford, 1990).

- <sup>32</sup>T. Huhne, C. Zecha, H. Ebert, P. H. Dederichs, and R. Zeller, Phys. Rev. B **58**, 10 236 (1998).
- <sup>33</sup>R. Podloucky, R. Zeller, and P. H. Dederichs, Phys. Rev. B **22**, 5777 (1980).
- <sup>34</sup>A. Abragam, *The Principles of Nuclear Magnetism* (Oxford University Press, Oxford, 1961).
- <sup>35</sup>O. Gunnarsson, J. Phys. F: Met. Phys. **6**, 587 (1976).
- <sup>36</sup>W. Götz and H. Winter, J. Phys.: Condens. Matter **5**, 1707 (1993).
- <sup>37</sup>P. Blaha, K. Schwarz, and P. H. Dederichs, Phys. Rev. B **37**, 2792 (1988).
- <sup>38</sup>H. Akai (private communication).
- <sup>39</sup>T. Funk, E. Beck, W. D. Brewer, C. Bobek, and E. Klein, J. Magn. Magn. Mater. **195**, 406 (1999).
- <sup>40</sup>H. Ebert, R. Zeller, B. Drittler, and P. H. Dederichs, J. Appl. Phys. **67**, 4576 (1990).
- <sup>41</sup>M. Weger, Phys. Rev. **128**, 1505 (1962).
- <sup>42</sup>C. Bobek, R. Dullenbacher, and E. Klein, Hyperfine Interact. **77**, 327 (1993).
- <sup>43</sup>E. Beck, W. D. Brewer, T. Funk, C. Bobek, and E. Klein, Aust. J. Phys. **51**, 281 (1998).
- <sup>44</sup>M. Kontani, T. Hioki, and Y. Masuda, J. Phys. Soc. Jpn. **32**, 416 (1972).
- <sup>45</sup>E. Klein, Hyperfine Interact. **15/16**, 557 (1983).